

A More Stable Accelerated Gradient Method Inspired by Continuous-Time Perspective

Yasong Feng* Weiguo Gao†

Abstract

Nesterov’s accelerated gradient method (NAG) is widely used in problems with machine learning background including deep learning, and is corresponding to a continuous-time differential equation. From this connection, the property of the differential equation and its numerical approximation can be investigated to improve the accelerated gradient method. In this work we present a new improvement of NAG in terms of stability inspired by numerical analysis. We give the precise order of NAG as a numerical approximation of its continuous-time limit and then present a new method with higher order. We show theoretically that our new method is more stable than NAG for large step size. Experiments of matrix completion and handwriting digit recognition demonstrate that the stability of our new method is better. Furthermore, better stability leads to higher computational speed in experiments.

1 Introduction

Optimization is a core component of statistic and machine learning problems. Recently, gradient-based algorithms are widely used in such optimization problems due to its simplicity and efficiency for large-scale situations. For solving convex optimization problem

$$\min_{x \in \mathbb{R}^d} F(x),$$

where $F(x)$ is convex with Lipschitz gradient, it is known that the objective function converges at a rate of $\mathcal{O}(n^{-1})$ when applying vanilla gradient descent.

Alternatively, Nesterov [1983] provided a more efficient first-order algorithm than gradient descent, which may take the following form: starting with $x_0 = x_1$,

$$\begin{aligned} y_n &= x_n + \frac{n-3}{n}(x_n - x_{n-1}), \\ x_{n+1} &= y_n - s\nabla F(y_n) \end{aligned} \tag{1.1}$$

for $n \geq 1$. It is shown that under abovementioned conditions, Nesterov’s accelerated gradient method (NAG) converges at the optimal rate $\mathcal{O}(n^{-2})$.

Accelerated gradient method has been successful in training deep and recurrent neural networks [Sutskever et al., 2013] and is widely used in problems with machine learning background to avoid

*ysfeng20@fudan.edu.cn

†wggao@fudan.edu.cn

sophisticated second-order methods [Hu et al., 2009, Ji and Ye, 2009, Cotter et al., 2011]. To provide more theoretical understanding, an important research topic of NAG is to find an explanation of the acceleration. Su et al. [2016] took the step size $s \rightarrow 0$ and showed that the continuous-time limit of NAG is the following ODE

$$\ddot{x} + \frac{3}{t}\dot{x} + \nabla F(x) = 0. \quad (1.2)$$

This differential equation was used as a tool for analyzing and generalizing Nesterov’s scheme. From this continuous-time perspective, progresses have been made in presenting new continuous frameworks, for example, see Wibisono et al. [2016], Wilson et al. [2016], Shi et al. [2018] and França et al. [2020a]. These new frameworks give more insight on the acceleration phenomenon. Furthermore, discretization methods are provided to derive optimization algorithms from a certain continuous-time framework. Zhang et al. [2018] showed that discrete the ODE (1.2) using a Runge-Kutta integrator can achieve acceleration. Shi et al. [2019] showed that applying symplectic scheme to a “high-resolution” version of limit ODE can also achieve acceleration. França et al. [2020b] presented a new method by discretizing a “dissipative relativistic system” that can be viewed as a generalization of NAG and heavy ball method.

Despite the successful use in practice, Nesterov’s accelerated gradient method is relatively poor in stability, that is, it requires a small step size to ensure convergence when applied to an objective function with large gradients [Lucas et al., 2019, França et al., 2020b], which limits the computational speed. To improve the stability, we present a new method motivated by numerical analysis. We prove that NAG is actually a numerical approximation of ordinary differential equation (1.2), so the properties in numerical analysis can be adopted to improve it. The order of a numerical approximation method is closely related with its stability. For example, the absolutely stable region of Runge-Kutta method is enlarged when the order is increased from one to four [Griffiths and Higham, 2010]. In this work we give the precise order of Nesterov’s accelerated gradient method as a numerical approximation of the limit ODE. Then inspired by the abovementioned property of Runge-Kutta method, we present a new higher order method (Algorithm 1), which we call *stabilized accelerated gradient* (SAG). Compared with NAG, we use one more step to calculate the starting point \mathbf{Y}_k for every iteration, so our SAG approximates the ordinary differential equation (1.2) better. We emphasize here that in many cases (including the two experiments in our work), the most computationally expensive step in gradient-based algorithms is the calculation of the gradients, so our modification will not cause inefficiency. Moreover, using absolute stability theory, we prove that our SAG is more stable than Nesterov’s method.

Based on abovementioned theoretical results, we try to take advantage of the new method in more practical problems. We apply SAG to a large-scale matrix completion problem. We combine SAG with proximal operator [Parikh and Boyd, 2014] into a new algorithm, which we call SFISTA. We show that the performance of our SFISTA is better than FISTA [Beck and Teboulle, 2009] and accelerated proximal gradient method [Parikh and Boyd, 2014] because of its better stability.

Furthermore, we show the advantage of our SAG by a handwriting digit recognition task. We train a convolutional neural network using SAG and NAG on *MNIST* [LeCun et al., 1998b] dataset. This experiment also verifies that our SAG is more stable with large step size.

This paper is organized as follows. In section 2, We prove that NAG is a numerical approximation of ordinary differential equation (1.2) and give the precise order. In section 3, we present our higher order method SAG and prove its better stability. In section 4 and 5, we apply our SAG to matrix completion and handwriting digit recognition tasks.

Algorithm 1 Stabilized Accelerated Gradient (SAG)

Input: step size s .

Initial value: $\mathbf{X}_2 = \mathbf{X}_1 = \mathbf{X}_0$.

$(k - 1)$ th iteration ($k \geq 2$). Compute

$$\begin{aligned}\mathbf{Y}_k &= \frac{10k^2 + 9k + 6}{4k^2 + 8k} \mathbf{X}_k - \frac{4k^2 + 3}{2k^2 + 4k} \mathbf{X}_{k-1} + \frac{2k - 1}{4k + 8} \mathbf{X}_{k-2}, \\ \mathbf{Z}_k &= \frac{2k - 3}{k} \mathbf{X}_k - \frac{k - 3}{k} \mathbf{X}_{k-1}, \\ \mathbf{X}_{k+1} &= \mathbf{Y}_k - \frac{ks}{2k + 4} \nabla F(\mathbf{Z}_k).\end{aligned}$$

2 The precise order of Nesterov's method as a numerical approximation of its continuous-time limit

We refer to $x(t)$ as the solution of differential equation (1.2). Su et al. [2016] proved the existence and uniqueness of such a solution. In this section, We give the precise order of NAG as a numerical approximation of $x(t)$.

We substitute the first equation in Nesterov's scheme (1.1) to the second one and substitute the relation $s = h^2$ to get

$$x_{n+1} = x_n + \frac{n-3}{n}(x_n - x_{n-1}) - h^2 \cdot \nabla F \left(x_n + \frac{n-3}{n}(x_n - x_{n-1}) \right). \quad (2.1)$$

Inspired by the ansatz $x_n \approx x(n\sqrt{s}) = x(nh)$ [Su et al., 2016], we consider the convergence between x_n and $x(nh)$. More precisely, we show that for fixed time t , x_n converges to $x(t)$ with order $\mathcal{O}(h \ln \frac{1}{h})$, where $n = \frac{t}{h}$.

2.1 Truncation error

Firstly, we consider the following "truncation error":

$$\begin{aligned}L[x(t); h] &= x(t+h) - \frac{2t-3h}{t}x(t) + \frac{t-3h}{t}x(t-h) + \\ &\quad h^2 \nabla F \left(x(t) + \frac{t-3h}{t}(x(t) - x(t-h)) \right).\end{aligned} \quad (2.2)$$

(2.2) is obtained from (2.1) by replacing x_{n+1} , x_n , x_{n-1} with $x(t+h)$, $x(t)$, $x(t-h)$ and substituting the relation $n = \frac{t}{h}$. Our first result is the order of truncation error $L[x(t); h]$.

Theorem 1. *Assume ∇F satisfies L -Lipschitz condition, and solution $x(t)$ of the derived differential equation (1.2) has a continuous third derivative. For fixed time t , the truncation error (2.2) satisfies*

$$L[x(t); h] = \mathcal{O}(h^3).$$

2.2 Approximation theorem

Theorem 1 coincides with derivation of ODE (1.2) [Su et al., 2016] and shows the size of error caused by a single iteration when the starting point is just on $x(t)$. Then we add up these errors to give the precise order of x_n converging to its limit dynamic system.

Theorem 2. *Under conditions in Theorem 1, for fixed time t and $n = t/h$, x_n converges to $x(t)$ at a rate of $\mathcal{O}(h \ln \frac{1}{h})$ if $x_0 = x(0)$ and $x_1 = x(h)$.*

For the proof of Theorem 2, we need the following two lemmas.

Lemma 1. [Holte, 2009] *For constant $\alpha, \beta > 0$ and positive sequence $\{\eta_n\}_{n \geq 0}$ satisfying*

$$\eta_n \leq \beta + \alpha \sum_{i=0}^{n-1} \eta_i, \quad \forall n > 0,$$

the following inequality holds

$$\eta_n \leq e^{\alpha n} (\beta + \alpha \eta_0).$$

The above lemma is a classic result and referred to as discrete Gronwall inequality.

Lemma 2. *We define matrices C_n and $D_{n,l}$ as*

$$C_n = \begin{pmatrix} \frac{2n-1}{n+1} & -\frac{n-2}{n+1} \\ 1 & 0 \end{pmatrix},$$

$$D_{n,l} = C_n C_{n-1} \cdots C_{n-l+1},$$

where $n \geq 0$ and $0 < l \leq n+1$. In addition, we set $D_{n,0} = \mathbf{I}_2$. Then there exist positive constants M, M_3 such that for all n , the following two inequalities hold, where the matrix norm is 2-norm.

$$\sup_{0 \leq l \leq n+1} \|D_{n,l}\| \leq Mn,$$

$$D_{n,n+1} \leq M_3.$$

The proof of Theorem 1, Lemma 2 and Theorem 2 are presented in Appendix A, B and C. We notice that Su et al. [2016] also presented an approximation result (Theorem 2 in Su et al. [2016]). However, our new approach is based on the order of truncation error and follows the classical path in numerical analysis that from consistence to convergence. This approach allows us to present the precise order of NAG as an approximation of the limit ODE, which is new to our knowledge. Based on this new result, we present our higher order method.

3 Stabilized accelerated gradient method

From Theorem 2, NAG can be viewed as a numerical approximation of the limit ODE (1.2). Therefore, the property of this limit differential equation and its numerical approximation can be investigated to improve the accelerated gradient method. In this section, we present a new way to improve the stability of NAG. It is well known that the absolutely stable region of Runge-Kutta method is enlarged when the order increases from one to four. Inspired by this fact, we present our new higher order method SAG. Here we show the derivation of SAG and then prove that our SAG is more stable than NAG.

3.1 Derivation of the new method and analysis of truncation error

We consider a recurrence relation with the following form

$$\sum_{i=1}^4 \left(\alpha_i + \frac{\beta_i}{n} + \frac{\gamma_i}{n^2} \right) x_{n+2-i} = -h^2 \nabla F \left(x_n + \frac{n-3}{n} (x_n - x_{n-1}) \right),$$

where $\{\alpha_i\}$, $\{\beta_i\}$ and $\{\gamma_i\}$ are to be determined. For this scheme, the truncation error becomes

$$\begin{aligned} L[x(t); h] &= \sum_{i=1}^4 \left(\alpha_i + \frac{\beta_i h}{t} + \frac{\gamma_i h^2}{t^2} \right) x(t + (2-i)h) \\ &\quad + h^2 \nabla F \left(x(t) + \frac{t-3h}{t} (x(t) - x(t-h)) \right). \end{aligned}$$

For the gradient term, we expand $x(t-h)$ to first order to get

$$\begin{aligned} \nabla F \left(x(t) + \frac{t-3h}{t} (x(t) - x(t-h)) \right) &= -hx^{(3)}(t) - \left(\frac{3h}{t} + 1 \right) x^{(2)}(t) \\ &\quad + \left(\frac{3h}{t^2} - \frac{3}{t} \right) x^{(1)}(t) + \mathcal{O}(h^2). \end{aligned}$$

Then we substitute this expansion for the gradient term in the truncation error. Calculation shows that the terms with order less than four of the truncation error will be eliminated if and only if the following equations are satisfied,

$$\begin{cases} \alpha_1 = 2 \\ \alpha_2 = -5 \\ \alpha_3 = 4 \\ \alpha_4 = -1 \end{cases}, \quad \begin{cases} \beta_1 = \frac{9}{2} - k \\ \beta_2 = -6 + 3k \\ \beta_3 = \frac{3}{2} - 3k \\ \beta_4 = k \end{cases}, \quad \begin{cases} \gamma_1 = m_1 \\ \gamma_2 = -\frac{3m_1 + m_2 + 3}{2} \\ \gamma_3 = m_2 \\ \gamma_4 = \frac{m_1 - m_2 + 3}{2} \end{cases},$$

where k , m_1 , m_2 can be chosen randomly. Then we set $k = \frac{1}{2}$, $m_1 = 0$ and $m_2 = 3$ to get our *stabilized accelerated gradient method* (Algorithm 1)

$$\begin{aligned} x_{n+1} &= \frac{10n^2 + 9n + 6}{4n^2 + 8n} x_n - \frac{4n^2 + 3}{2n^2 + 4n} x_{n-1} + \frac{2n-1}{4n+8} x_{n-2} \\ &\quad - \frac{n}{2n+4} h^2 \nabla F \left(\frac{2n-3}{n} x_n - \frac{n-3}{n} x_{n-1} \right). \end{aligned} \tag{3.1}$$

For truncation order of SAG, we have the following theorem. The abovementioned procedure is presented in detail in Appendix D, as proof of Theorem 3.

Theorem 3. *If ∇F has continuous second order derivative, the first and second derivative are bounded, and $x(t)$ has continuous fourth derivative, then for fixed t , truncation error of SAG (3.1) satisfies*

$$L[x(t); h] = \mathcal{O}(h^4).$$

3.2 Better stability of SAG

In this subsection, we verify the better stability of the new method. The stability here refers to the feasible region of step size. It is shown that step size should be chosen in absolute stable region to ensure stable performance of the algorithm [Leader, 2004]. Therefore, a more stable method should have a larger absolute stable region, so that its effectiveness is ensured when the step size is large. We emphasize here that since absolute stable theory is corresponding to accumulated error, it can be widely used in iterative algorithms, although this concept was originally proposed for numerical integrators. Similar analyses are applied to different optimization methods in Su et al. [2016] and França et al. [2020b].

Firstly, recall the scheme of SAG

$$x_{n+1} = \frac{10n^2 + 9n + 6}{4n^2 + 8n}x_n - \frac{4n^2 + 3}{2n^2 + 4n}x_{n-1} + \frac{2n - 1}{4n + 8}x_{n-2} - \frac{n}{2n + 4}s\nabla F\left(\frac{2n - 3}{n}x_n - \frac{n - 3}{n}x_{n-1}\right).$$

We use notations $\mathbf{X}_{n+1} = (x_{n+1}, x_n, x_{n-1})^\top$ and $\mathbf{X}_n = (x_n, x_{n-1}, x_{n-2})^\top$, then the scheme can be written as

$$\mathbf{X}_{n+1} = F^{(n)}(\mathbf{X}_n) = \begin{pmatrix} F_1^{(n)}(\mathbf{X}_n) \\ F_2^{(n)}(\mathbf{X}_n) \\ F_3^{(n)}(\mathbf{X}_n) \end{pmatrix},$$

where $F_1^{(n)}(x, y, z) = \frac{10n^2 + 9n + 6}{4n^2 + 8n}x - \frac{4n^2 + 3}{2n^2 + 4n}y + \frac{2n - 1}{4n + 8}z - \frac{n}{2n + 4}s\nabla F\left(\frac{2n - 3}{n}x - \frac{n - 3}{n}y\right)$, $F_2^{(n)}(x, y, z) = x$ and $F_3^{(n)}(x, y, z) = y$.

In a real SAG run, we calculate a numerical approximation $\bar{\mathbf{X}}_n$ of each \mathbf{X}_n in turn. Assume that there is an error $\mathbf{e} = (e_1, e_2, e_3)^\top$ between $\bar{\mathbf{X}}_n$ and \mathbf{X}_n . Then in the next iteration, we have

$$\bar{\mathbf{X}}_{n+1} = F^{(n)}(\bar{\mathbf{X}}_n) = \begin{pmatrix} F_1^{(n)}(\mathbf{X}_n + \mathbf{e}) \\ F_2^{(n)}(\mathbf{X}_n + \mathbf{e}) \\ F_3^{(n)}(\mathbf{X}_n + \mathbf{e}) \end{pmatrix}. \quad (3.2)$$

For the first entry of RHS, we have

$$\begin{aligned}
F_1^{(n)}(\mathbf{X}_n + \mathbf{e}) &= \frac{10n^2 + 9n + 6}{4n^2 + 8n}(x_n + e_1) - \frac{4n^2 + 3}{2n^2 + 4n}(x_{n-1} + e_2) + \frac{2n - 1}{4n + 8}(x_{n-2} + e_3) \\
&\quad - \frac{n}{2n + 4}s\nabla F \left(\frac{2n - 3}{n}(x_n + e_1) - \frac{n - 3}{n}(x_{n-1} + e_2) \right) \\
&\approx \frac{10n^2 + 9n + 6}{4n^2 + 8n}(x_n + e_1) - \frac{4n^2 + 3}{2n^2 + 4n}(x_{n-1} + e_2) + \frac{2n - 1}{4n + 8}(x_{n-2} + e_3) \\
&\quad - \frac{n}{2n + 4}s\nabla F \left(\frac{2n - 3}{n}x_n - \frac{n - 3}{n}x_{n-1} \right) \\
&\quad - \frac{n}{2n + 4}s\nabla^2 F \left(\frac{2n - 3}{n}x_n - \frac{n - 3}{n}x_{n-1} \right) \cdot \left(\frac{2n - 3}{n}e_1 - \frac{n - 3}{n}e_2 \right) \\
&= F_1^{(n)}(\mathbf{X}_n) + \left(\frac{10n^2 + 9n + 6}{4n^2 + 8n} - \frac{2n - 3}{2n + 4}s\nabla^2 F \right) e_1 - \left(\frac{4n^2 + 3}{2n^2 + 4n} - \frac{n - 3}{2n + 4}s\nabla^2 F \right) e_2 \\
&\quad + \frac{2n - 1}{4n + 8}e_3,
\end{aligned}$$

where in the second line we use Taylor approximation, and in the third line we use $\nabla^2 F$ to denote $\nabla^2 F \left(\frac{2n-3}{n}x_n - \frac{n-3}{n}x_{n-1} \right)$.

Then (3.2) implies that

$$\begin{aligned}
\bar{\mathbf{X}}_{n+1} &\approx \mathbf{X}_{n+1} + \begin{pmatrix} \left(\frac{10n^2 + 9n + 6}{4n^2 + 8n} - \frac{2n - 3}{2n + 4}s\nabla^2 F \right) & - \left(\frac{4n^2 + 3}{2n^2 + 4n} - \frac{n - 3}{2n + 4}s\nabla^2 F \right) & \frac{2n - 1}{4n + 8} \\ 1 & 0 & 0 \\ 0 & 1 & 0 \end{pmatrix} \begin{pmatrix} e_1 \\ e_2 \\ e_3 \end{pmatrix} \\
&\triangleq \mathbf{X}_{n+1} + \mathbf{P}\mathbf{e}.
\end{aligned}$$

The characteristic equation of matrix \mathbf{P} is

$$\lambda^3 - \left(\frac{10n^2 + 9n + 6}{4n^2 + 8n} - \frac{2n - 3}{2n + 4}s\nabla^2 F \right) \lambda^2 + \left(\frac{4n^2 + 3}{2n^2 + 4n} - \frac{n - 3}{2n + 4}s\nabla^2 F \right) \lambda - \frac{2n - 1}{4n + 8} = 0.$$

For large n , we ignore the high order terms and the characteristic equation becomes

$$\lambda^3 - \left(\frac{5}{2} - s \cdot \nabla^2 F \right) \lambda^2 + \left(2 - \frac{s}{2} \cdot \nabla^2 F \right) \lambda - \frac{1}{2} = 0. \quad (3.3)$$

According to the stability theory, the absolute stable region is the set of step size s such that all the roots of the characteristic equation (eigenvalues) lie in the unit circle [Leader, 2004]. Since the left hand of (3.3) can be factorized to

$$\left(\lambda - \frac{1}{2} \right) \left(\lambda^2 - (2 - s \cdot \nabla^2 F)\lambda + 1 \right),$$

this condition equals to $0 \leq s \cdot \nabla^2 F \leq 4$. In another word, the absolutely stable region of SAG is $\{s : s \cdot \nabla^2 F \in [0, 4]\}$.

We then consider NAG. Applying the same approximations, we get the characteristic equation of NAG

$$\lambda^2 - (2 - 2s \cdot \nabla^2 F)\lambda + (1 - s \cdot \nabla^2 F) = 0. \quad (3.4)$$

It is easy to verify that the absolutely stable region of NAG is $\{s : s \cdot \nabla^2 F \in [0, \frac{4}{3}]\}$. In summary, we have the following proposition.

Proposition 1. *Under abovementioned approximations, the characteristic equation of SAG and NAG are presented in (3.3) and (3.4). The absolutely stable region of SAG is $\{s : s \cdot \nabla^2 F \in [0, 4]\}$, while the absolutely stable region of NAG is $\{s : s \cdot \nabla^2 F \in [0, \frac{4}{3}]\}$.*

Remark 1. *If we change the choice of parameters k, m_1, m_2 in subsection 3.1 and so change the form of the new method, the absolutely stable region will remain unchanged.*

When s lies in the absolutely stable region, stability theory guarantees that errors will not be magnified during iteration. Proposition 1 shows that the absolutely stable region of SAG is larger than NAG, so our new method is more stable.

4 Application to matrix completion problem: SFISTA

Our SAG has a larger absolutely stable region than NAG, so we can choose larger step size when applying SAG and the computation will be faster. In this section we apply our SAG to matrix completion problem. We combine our SAG with proximal operator to present a new algorithm which can be viewed as a modification of the well-known fast iterative shrinkage-thresholding algorithm (FISTA) [Beck and Teboulle, 2009]. Then we show the better stability and higher computation speed of our new method by comparing with FISTA.

For matrix completion problem there exists a “true” low rank matrix \mathbf{M} . We are given some entries of \mathbf{M} and asked to fill missing entries. In our simulated dataset, the size of \mathbf{M} is 1000×1000 , and the true rank of \mathbf{M} is set to be 4. There have been various algorithms to solve such problem [Candès and Recht, 2009, Keshavan et al., 2010]. Besides, it is proposed that matrix completion can be transformed to the following unconstrained optimization problem [Mazumder et al., 2010]

$$\min_{\mathbf{X}} F(\mathbf{X}) = \frac{1}{2} \|\mathbf{X}_{obs} - \mathbf{M}_{obs}\|^2 + \lambda \|\mathbf{X}\|_*.$$

$F(\mathbf{X})$ is composed of a smooth term and a non-smooth term, so gradient-based algorithms cannot be used directly. Proximal gradient algorithms [Parikh and Boyd, 2014] are widely used in such composite optimization problems, and fast iterative shrinkage-thresholding algorithm (FISTA) is a successful algorithm. Moreover, FISTA has been extended to matrix completion case [Ji and Ye, 2009]. For convenience, we set $G(\mathbf{X}) = \frac{1}{2} \|\mathbf{X}_{obs} - \mathbf{M}_{obs}\|^2$, $H(\mathbf{X}) = \lambda \|\mathbf{X}\|_*$, and $g(\mathbf{X}) = \nabla G(\mathbf{X})$. The idea of FISTA builds on NAG. We also apply accelerated proximal gradient method (APG) [Parikh and Boyd, 2014] for our numerical experiment, which is composed of NAG and proximal gradient descent. These two algorithms are presented in Appendix E. We find the performances of them are similar in our experiments.

Our contribution is the third method (Algorithm 2), SAG combined with proximal operator, which we call SFISTA. Notice that the minimizing problems in iterations of above three algorithms can be solved directly by singular value decomposition [Cai and Candès, 2010].

Algorithm 2 SFISTA

Input: step size s .

Initial value: $\mathbf{X}_2 = \mathbf{X}_1 = \mathbf{X}_0 = \mathbf{M}_{obs}$.

$(k - 1)$ th iteration ($k \geq 2$). Compute

$$\begin{aligned}\mathbf{Y}_k &= \frac{10k^2 + 9k + 6}{4k^2 + 8k} \mathbf{X}_k - \frac{4k^2 + 3}{2k^2 + 4k} \mathbf{X}_{k-1} + \frac{2k - 1}{4k + 8} \mathbf{X}_{k-2}, \\ \mathbf{Z}_k &= \frac{2k - 3}{k} \mathbf{X}_k - \frac{k - 3}{k} \mathbf{X}_{k-1}, \\ \mathbf{X}_{k+1} &= \arg \min_{\mathbf{X}} \left\{ \frac{1}{2} \cdot \frac{2k + 4}{ks} \left\| \mathbf{X} - \left(\mathbf{Y}_k - \frac{ks}{2k + 4} g(\mathbf{Z}_k) \right) \right\|^2 + \lambda \|\mathbf{X}\|_* \right\}.\end{aligned}$$

In the above three algorithms, we use fixed step sizes, and the results are presented in the first four subfigures of Figure 1. During this experiment, our first find is that the range of step size that our SFISTA can converge stably is significantly larger than those of FISTA and APG. Experiment shows that the feasible regions of step size of FISTA and APG are both $(0, 1.4]$ (accurate to one decimal place), while that of our SFISTA is $(0, 4.5]$. Secondly, we find empirically that for all methods, convergence is faster when step size is larger (within the feasible region). Therefore, we choose the largest step sizes in the feasible region for all methods to compare their highest computational speed. We also compare performances of the three methods with step sizes reduced from the largest in equal proportion. We find that when step sizes are chosen to be the largest or reduced from the largest in equal proportion (80%, 50%, 10%), convergence of SFISTA is faster than the other two methods.

Furthermore, we combine the three methods with backtracking [Beck and Teboulle, 2009] to choose step sizes automatically. We present SFISTA with backtracking below (Algorithm 3), and the other two algorithms are similar (presented in Appendix E). Performances of the three algorithms with backtracking are compared on abovementioned dataset, and the result is shown in Figure 1(e). Convergence of SFISTA is faster than the other two methods. Moreover, we find that the step size of SAG is reduced 9 times during the 200 iterations, while step sizes of FISTA and APG are both reduced 13 times. This find also confirms the better stability of SFISTA.

In short, the better stability of SFISTA enables it to work well with larger step size than FISTA and APG, which also leads to faster computation.

5 Application to handwriting digit recognition

In this section, we evaluate SAG and NAG with handwriting digit recognition task. *MNIST* [LeCun et al., 1998b] is a large dataset of handwriting digits and is widely used in training and testing image recognition system. One of the most popular models to analyze visual imagery is convolutional neural network (CNN) [LeCun et al., 1998a]. Here we train a two-layer CNN by SAG and NAG on *MNIST* dataset and evaluate their performances.

MNIST dataset [LeCun et al., 1998b] contains 60000 training images and 10000 test images. In our experiment, we use the first 20000 images to train a two-layer convolutional neural network and use the whole 10000 images to test the accuracy of our network. The test accuracies during iteration

Algorithm 3 SFISTA with backtracking

Input: some $\beta < 1$.

Initial value: $\mathbf{X}_2 = \mathbf{X}_1 = \mathbf{X}_0 = \mathbf{M}_{obs}$, step size s_2 .

($k - 1$)th iteration ($k \geq 2$).

$$\begin{aligned}\mathbf{Y}_k &= \frac{10k^2 + 9k + 6}{4k^2 + 8k} \mathbf{X}_k - \frac{4k^2 + 3}{2k^2 + 4k} \mathbf{X}_{k-1} + \frac{2k - 1}{4k + 8} \mathbf{X}_{k-2}, \\ \mathbf{Z}_k &= \frac{2k - 3}{k} \mathbf{X}_k - \frac{k - 3}{k} \mathbf{X}_{k-1}.\end{aligned}$$

Find the smallest nonnegative integer i_{k+1} such that with $s = \beta^{i_{k+1}} s_k$

$$F(\widetilde{\mathbf{X}}) < F(\mathbf{Y}_k) + \left\langle \widetilde{\mathbf{X}} - \mathbf{Y}_k, g(\mathbf{Z}_k) \right\rangle + \frac{1}{2} \cdot \frac{2k + 4}{ks} \|\widetilde{\mathbf{X}} - \mathbf{Y}_k\|^2,$$

where

$$\widetilde{\mathbf{X}} = \arg \min_{\mathbf{X}} \left\{ \frac{1}{2} \cdot \frac{2k + 4}{ks} \left\| \mathbf{X} - \left(\mathbf{Y}_k - \frac{ks}{2k + 4} g(\mathbf{Z}_k) \right) \right\|^2 + \lambda \|\mathbf{X}\|_* \right\}.$$

Set $s_{k+1} = \beta^{i_{k+1}} s_k$ and compute

$$\mathbf{X}_{k+1} = \widetilde{\mathbf{X}}.$$

are provided in Figure 2. When the step size is relatively small (0.02 in the experiment), accuracies of both methods increase to more than 97% at similar speeds. When the step size is enlarged to 0.08, the accuracy curve of NAG is relatively unstable compared to our SAG. When the step size is large (0.14 in the experiment), accuracy of SAG can still increase to 97%, while NAG oscillates violently and fails to train a useful network. We find that our SAG has less oscillation than NAG, which also leads to larger feasible region of step size and faster convergence. This consists with our theoretical result and confirms the better stability of SAG. More detailed results of this experiment are presented in Appendix F.

To compare SAG and NAG more quantitatively, we take another experiment to evaluate the local performance of the two methods. Note that we use quadratic approximation in stability analysis. Therefore, due to the non-convexity of neural network objective function, the better performance of SAG is more significant when parameters of the network are not far from the optimal ones. More precisely, our training procedure consists of two steps:

1. Train the neural network with an approximate method until the test accuracy is not less than 90%.
2. Switch to optimizer SAG/NAG with step size s .

Then we compare the performance of SAG and NAG with different step size in step 2.

In the experiment, we randomly choose 5 different initial values and use NAG with sufficiently small step size (0.02) for step 1. For step 2, we apply SAG and NAG with 30 different step sizes (from 0.01 to 0.3 with gap 0.01), and measure the performance by the number of steps needed to gain a

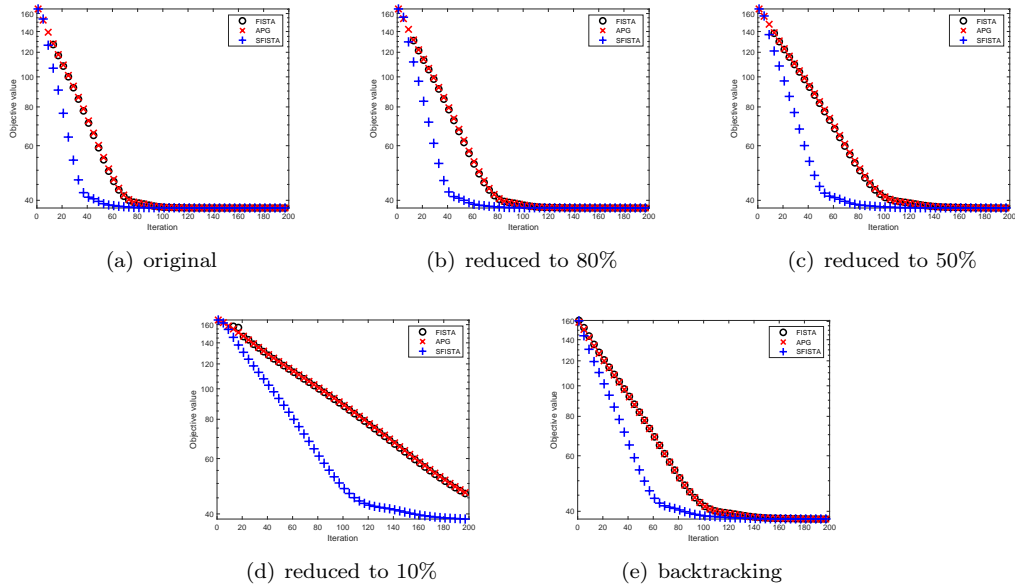


Figure 1: Iterations of FISTA, APG and SFISTA for matrix completion objective function. Y-axis represents the objective function $F(x_n)$. In Figure 1(a), step size is 1.4 for FISTA and APG, and 4.5 for SFISTA. In the next three figures, step sizes are reduced from 1.4 and 4.5 in the proportion marked below the figures. In Figure 1(e), step sizes are chosen automatically by backtracking.

loss value less than 0.1. In Table 1, we record the best choices of step size for different initial values and algorithms. It is obvious the best step size of SAG is about two times as large as that of NAG. We also present the number of steps needed with the best step size for different initial values and algorithms in table 2. The results show that our SAG is about 1.6 times faster than NAG in step 2.

Algorithm	Init.1	Init.2	Init.3	Init. 4	Init. 5
SAG	0.26	0.19	0.07	0.24	0.15
NAG	0.13	0.1	0.04	0.11	0.08

Table 1: Best choice of step size for SAG and NAG.

6 Discussion

In this paper we give the precise order of NAG as a numerical approximation of the limit differential equation. Inspired by this perspective, we present a new method which we call *stabilized accelerated gradient* (SAG).

We prove that our SAG has a larger absolutely stable region, so it works more stable with large step size. We evaluate the performance of SAG in two experiments: matrix completion and handwriting

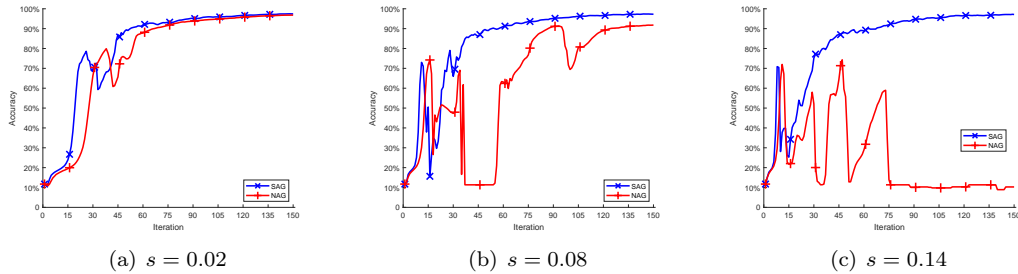


Figure 2: Iterations of SAG and NAG for test accuracy. Y-axis represents the test accuracies for both methods. Step size is 0.02 in Figure 2(a), 0.08 in Figure 2(b) and 0.14 in Figure 2(c).

Algorithm	Init.1	Init.2	Init.3	Init. 4	Init. 5
SAG	28	32	41	27	31
NAG	48	53	56	51	46

Table 2: Minimum number of steps needed to achieve 0.1 loss for SAG and NAG.

digit recognition. In both experiments, we find that our SAG has a larger region of feasible step size than NAG, which confirms the better stability of SAG. Moreover, better stability of SAG leads to higher computational speed.

In summary, we provide a new way to improve the stability of Nesterov’s accelerated gradient method, and our approach indicates how properties in numerical analysis can be used to refine an optimization method. We believe this approach is worth further study and more higher order methods may be worth considering. Finally, more theoretical analysis of SAG is still a future topic. From previous paper and this work we know that the limit ODE (1.2) converges to the minimum at a speed $\mathcal{O}(t^{-2})$ [Su et al., 2016] (coincides with $\mathcal{O}(n^{-2})$ of NAG) and SAG is a better approximation of the ODE than Nesterov’s method. These two facts imply the $\mathcal{O}(n^{-2})$ convergence of SAG, which is also verified by the better performance of SAG in practice. However, a direct convergence analysis is to be involved. This analysis might be finished by technical construction of estimate sequence. Furthermore, it would be interesting to apply SAG to deep neural network, especially to a landscape with large gradient.

References

- Amir Beck and Marc Teboulle. A fast iterative shrinkage-thresholding algorithm for linear inverse problems. *SIAM Journal on Imaging Sciences*, 2(1):183–202, 2009.
- Jianfeng Cai and Emmanuel J. Candès. A singular value thresholding algorithm for matrix completion. *SIAM Journal on Optimization*, 20(4):1956–1982, 2010.
- Emmanuel J. Candès and Benjamin Recht. Exact matrix completion via convex optimization. *Foundations of Computational Mathematics*, 9(6):717–772, 2009.

- Andrew Cotter, Ohad Shamir, Nati Srebro, and Karthik Sridharan. Better mini-batch algorithms via accelerated gradient methods. *Advances in Neural Information Processing Systems 24*, pages 1647–1655, 2011.
- Guilherme França, Michael I Jordan, and René Vidal. On dissipative symplectic integration with applications to gradient-based optimization. *arXiv preprint arXiv:2004.06840*, 2020a.
- Guilherme França, Jeremias Sulam, Daniel Robinson, and René Vidal. Conformal symplectic and relativistic optimization. *Advances in Neural Information Processing Systems 33*, pages 16916–16926, 2020b.
- David F. Griffiths and Desmond J. Higham. *Numerical Methods for Ordinary Differential Equations: Initial Value Problems*. Springer Science & Business Media, 2010.
- John M. Holte. Discrete Gronwall lemma and applications. *MAA-NCS meeting at the University of North Dakota*, 2009.
- Chonghai Hu, Weike Pan, and James T. Kwok. Accelerated gradient methods for stochastic optimization and online learning. *Advances in Neural Information Processing Systems 22*, pages 781–789, 2009.
- Shuiwang Ji and Jiepeng Ye. Exact matrix completion via convex optimization. *Proceedings of the 26th International Conference on Machine Learning*, pages 457–464, 2009.
- Raghunandan H. Keshavan, Andrea Montanari, and Sewoong Oh. Matrix completion from a few entries. *IEEE Transactions on Information Theory*, 56(6):2980–2998, 2010.
- Jeffery J. Leader. *Numerical Analysis and Scientific Computation*. Pearson Addison Wesley, 2004.
- Yann LeCun, Léon Bottou, Yoshua Bengio, and Patrick Haffner. Gradient-based learning applied to document recognition. *Proceedings of the IEEE*, 86(11):2278–2324, 1998a.
- Yann LeCun, Corinna Cortes, and Christopher J.C. Burges. The MNIST database of handwritten digits. <http://yann.lecun.com/exdb/mnist/>, 1998b.
- James Lucas, Shengyang Sun, Richard Zemel, and Roger Grosse. Aggregated momentum: stability through passive damping. *International Conference on Learning Representations (ICLR)*, 2019.
- Rahul Mazumder, Trevor Hastie, and Robert Tibshirani. Spectral regularization algorithms for learning large incomplete matrices. *The Journal of Machine Learning Research*, 11:2287–2322, 2010.
- Yurii E. Nesterov. A method for solving the convex programming problem with convergence rate $\mathcal{O}(k^{-2})$. *Soviet Mathematics Doklady*, 27(2):372–376, 1983.
- Neal Parikh and Stephen Boyd. Proximal algorithms. *Foundations and Trends in Optimization*, 1(3):127–239, 2014.
- Bin Shi, Simon S Du, Michael I Jordan, and Weijie Su. Understanding the acceleration phenomenon via high-resolution differential equations. *arXiv preprint arXiv:1810.08907*, 2018.

- Bin Shi, Simon S Du, Weijie Su, and Michael I Jordan. Acceleration via symplectic discretization of high-resolution differential equations. *Advances in Neural Information Processing Systems 32*, pages 5745–5753, 2019.
- Weijie Su, Stephen Boyd, and Emmanuel J. Candès. A differential equation for modeling Nesterov’s accelerated gradient method: Theory and insights. *The Journal of Machine Learning Research*, 17(1):5312–5354, 2016.
- Ilya Sutskever, James Martens, George Dahl, and Geoffrey Hinton. On the importance of initialization and momentum in deep learning. *Proceedings of the 30th International Conference on Machine Learning*, pages 1139–1147, 2013.
- Andre Wibisono, Ashia C. Wilson, and Michael I. Jordan. A variational perspective on accelerated methods in optimization. *Proceedings of the National Academy of Sciences*, 113(47):E7351–E7358, 2016.
- Ashia C Wilson, Benjamin Recht, and Michael I Jordan. A Lyapunov analysis of momentum methods in optimization. *arXiv preprint arXiv:1611.02635*, 2016.
- Jingzhao Zhang, Aryan Mokhtari, Suvrit Sra, and Ali Jadbabaie. Direct Runge-Kutta discretization achieves acceleration. *Advances in Neural Information Processing Systems 31*, pages 3900–3909, 2018.

A Proof of Theorem 1

Theorem 1. Assume ∇F satisfies L -Lipschitz condition, and solution $x(t)$ of the derived differential equation (1.2) has a continuous third derivative. For fixed time t , the truncation error (2.2) satisfies

$$L[x(t); h] = \mathcal{O}(h^3). \tag{A.1}$$

Proof. We substitute the equality

$$x(t - h) = x(t) + \mathcal{O}(h)$$

to the last term of

$$L[x(t); h] = x(t + h) - \frac{2t - 3h}{t}x(t) + \frac{t - 3h}{t}x(t - h) + h^2 \nabla F \left(x(t) + \frac{t - 3h}{t} (x(t) - x(t - h)) \right) \tag{A.2}$$

to get

$$\nabla F \left(x(t) + \frac{t - 3h}{t} (x(t) - x(t - h)) \right) = \nabla F \left(x(t) + \frac{t - 3h}{t} \cdot \mathcal{O}(h) \right).$$

Since ∇F satisfies L -Lipschitz condition, we know

$$\begin{aligned} \nabla F \left(x(t) + \frac{t - 3h}{t} (x(t) - x(t - h)) \right) &= \nabla F(x(t)) + \mathcal{O}(h) \\ &= -x^{(2)}(t) - \frac{3}{t}x^{(1)}(t) + \mathcal{O}(h). \end{aligned}$$

For the second equality, we substitute the differential equation (1.2). Then we expand the first and third terms of $L[x(t); h]$ to third order

$$\begin{aligned} x(t+h) &= x(t) + hx^{(1)}(t) + \frac{h^2}{2}x^{(2)}(t) + \mathcal{O}(h^3), \\ x(t-h) &= x(t) - hx^{(1)}(t) + \frac{h^2}{2}x^{(2)}(t) + \mathcal{O}(h^3). \end{aligned}$$

Finally, we substitute these three equations to the truncation error (A.2) to conclude

$$L[x(t); h] = \mathcal{O}(h^3). \quad \square$$

Remark 2. (A.1) can be written as

$$|L[x(t); h]| \leq M_0 h^3,$$

where M_0 depends on $\sup_{s \leq t} |x^{(1)}(s)|$ and $\sup_{s \leq t} |x^{(3)}(s)|$.

Remark 3. Theorem 1 deals with the problem for fixed time t . To finish the proof of the approximation theorem, we have to consider the situation that $t_n = nh$, where $n \geq 1$ is fixed.

We set a fixed time t_0 and assume that $t_n = nh < t_0$. Since $x(t)$ has a continuous third derivative, $x(t)$ and its first to third derivative are bounded in $[0, t_0]$. We replace time t in the above proof by t_n and expand the terms of (A.2). Now the term

$$-\frac{3h^3}{2t_n}x^{(2)}(t_n)$$

obtained from the expansion of $x(t_n - h)$ cannot be viewed as $\mathcal{O}(h^3)$, but there exists $M_2 > 0$ such that

$$\left| -\frac{3h^3}{2t_n}x^{(2)}(t_n) \right| \leq M_2 \frac{h^2}{n}.$$

As a consequence, we have

$$|L[x(t_n); h]| \leq M_1 h^3 + M_2 \frac{h^2}{n}, \quad (\text{A.3})$$

where M_1 and M_2 rely on t_0 .

B Proof of Lemma 2

Lemma 2. We define matrices \mathbf{C}_n and $\mathbf{D}_{n,l}$ as

$$\begin{aligned} \mathbf{C}_n &= \begin{pmatrix} \frac{2n-1}{n+1} & -\frac{n-2}{n+1} \\ 1 & 0 \end{pmatrix}, \\ \mathbf{D}_{n,l} &= \mathbf{C}_n \mathbf{C}_{n-1} \cdots \mathbf{C}_{n-l+1}, \end{aligned}$$

where $n \geq 0$ and $0 < l \leq n+1$. In addition, we set $\mathbf{D}_{n,0} = \mathbf{I}_2$. Then there exist positive constants M , M_3 such that for all n , the following two inequalities hold, where the matrix norm is 2-norm.

$$\sup_{0 \leq l \leq n+1} \|\mathbf{D}_{n,l}\| \leq Mn, \quad (\text{B.1})$$

$$\mathbf{D}_{n,n+1} \leq M_3. \quad (\text{B.2})$$

Proof. From

$$\mathbf{C}_2 = \begin{pmatrix} 1 & 0 \\ 1 & 0 \end{pmatrix},$$

we have

$$\mathbf{D}_{n,n-1} = \begin{pmatrix} 1 & 0 \\ 1 & 0 \end{pmatrix}, \quad \mathbf{D}_{n,n} = \begin{pmatrix} \frac{1}{2} & \frac{1}{2} \\ \frac{1}{2} & \frac{1}{2} \end{pmatrix}, \quad \mathbf{D}_{n,n+1} = \begin{pmatrix} 0 & 1 \\ 0 & 1 \end{pmatrix},$$

for $n \geq 2$. So it is obvious that there exists M_3 to make (B.2) true and $M_4 > 0$ such that for all $n < 2$ or $n \geq 2$, $l > n - 2$ or $l = 0$,

$$\|\mathbf{D}_{n,l}\| \leq M_4 n. \quad (\text{B.3})$$

Then we consider the situation of $n \geq 2$, $0 < l \leq n - 2$. Notice that

$$\mathbf{C}_n = \mathbf{P} \begin{pmatrix} 1 & 1 \\ 0 & \frac{n-2}{n+1} \end{pmatrix} \mathbf{P}^{-1},$$

where

$$\mathbf{P} = \begin{pmatrix} 1 & 1 \\ 1 & 0 \end{pmatrix}.$$

Assume we have already got

$$\mathbf{D}_{n,l} = \mathbf{P} \begin{pmatrix} 1 & a_{n,l} \\ 0 & b_{n,l} \end{pmatrix} \mathbf{P}^{-1}$$

satisfying

$$0 < a_{n,l} \leq l, \quad 0 < b_{n,l} \leq 1.$$

Then since

$$\mathbf{D}_{n,l+1} = \mathbf{D}_{n,l} \mathbf{C}_{n-l} \quad \text{and} \quad 0 \leq \frac{n-l-2}{n-l+1} < 1,$$

$\mathbf{D}_{n,l+1}$ can be written as

$$\mathbf{D}_{n,l+1} = \mathbf{P} \begin{pmatrix} 1 & a_{n,l+1} \\ 0 & b_{n,l+1} \end{pmatrix} \mathbf{P}^{-1},$$

where

$$0 < a_{n,l+1} \leq l+1, \quad 0 < b_{n,l} \leq 1.$$

Then for fixed n , we induce from $l = 1$ to get

$$\mathbf{D}_{n,l} = \mathbf{P} \tilde{\mathbf{D}}_{n,l} \mathbf{P}^{-1} \triangleq \mathbf{P} \begin{pmatrix} 1 & a_{n,l} \\ 0 & b_{n,l} \end{pmatrix} \mathbf{P}^{-1},$$

where

$$0 < a_{n,l} \leq l \leq n, \quad 0 < b_{n,l} \leq 1, \quad (\text{B.4})$$

for all $n \geq 2$, $0 < l \leq n - 2$. Then we can estimate $\|\mathbf{D}_{n,l}\|$. Calculation shows that

$$\tilde{\mathbf{D}}_{n,l} \tilde{\mathbf{D}}_{n,l}^\top = \begin{pmatrix} 1 + a_{n,l}^2 & a_{n,l} b_{n,l} \\ a_{n,l} b_{n,l} & a_{n,l}^2 \end{pmatrix}.$$

The eigenvalues of this matrix are

$$\lambda_{1,2} = \frac{1 + a_{n,l}^2 + b_{n,l}^2 \pm \sqrt{(1 + a_{n,l}^2 + b_{n,l}^2)^2 - 4b_{n,l}^4}}{2}.$$

Combining this representation with (B.4), we get the estimation

$$\|\tilde{\mathbf{D}}_{n,l}\| = \sqrt{\max\{|\lambda_1|, |\lambda_2|\}} \leq \sqrt{1 + a_{n,l}^2 + b_{n,l}^2} \leq n + 2.$$

So there exists $M_5 > 0$, such that for all $n \geq 2$, $0 < l \leq n - 2$, inequality

$$\|\mathbf{D}_{n,l}\| \leq M_5 n \tag{B.5}$$

holds. Combining (B.3) with (B.5), we finish the proof of (B.1). \square

C Proof of Theorem 2

Theorem 2. Under conditions in Theorem 1, for fixed time t and $n = t/h$, x_n converges to $x(t)$ at a rate of $\mathcal{O}(h \ln \frac{1}{h})$ if $x_0 = x(0)$ and $x_1 = x(h)$.

Proof. In this proof, we first calculate the error caused by a single iteration, which can be divided into an accumulation term and a truncation term. Then we use the error estimation given by Theorem 1 and apply discrete Gronwall inequality to prove the convergence.

The difference of our situation from classic situation in numerical analysis is that the iteration scheme changes with n , so the classic technique can not be used to bound the norm of the transition matrix and the truncation error. Our new approach is presented in Remark 3 of Theorem 1 and Lemma 2, and is the most important technical innovation in our proof.

Recall the recurrence relation

$$x_{n+1} = x_n + \frac{n-3}{n}(x_n - x_{n-1}) - h^2 \nabla F \left(x_n + \frac{n-3}{n}(x_n - x_{n-1}) \right)$$

and the definition of truncation error

$$x(t_{n+1}) = x(t_n) + \frac{n-3}{n}(x(t_n) - x(t_{n-1})) - h^2 \nabla F \left(x(t_n) + \frac{n-3}{n}(x(t_n) - x(t_{n-1})) \right) + L[x(t_n); h],$$

where $t_n = nh$.

We subtract the above two equations, and introduce overall error

$$e_n = x(t_n) - x_n$$

to get

$$e_{n+1} = \frac{2n-3}{n}e_n - \frac{n-3}{n}e_{n-1} - h^2 b_{n-1} + L[x(t_n); h],$$

which can also be written as

$$e_{n+2} - \frac{2n-1}{n+1}e_{n+1} + \frac{n-2}{n+1}e_n = -h^2 b_n + L[x(t_{n+1}); h], \tag{C.1}$$

where

$$b_n = \nabla F \left(\frac{2n-1}{n+1}x_{n+1} - \frac{n-2}{n+1}x_n \right) - \nabla F \left(\frac{2n-1}{n+1}x(t_{n+1}) - \frac{n-2}{n+1}x(t_n) \right). \tag{C.2}$$

Then we rewrite (C.1) into a form that is convenient for recurrence. We set

$$\mathbf{E}_n = \begin{pmatrix} e_{n+1} \\ e_n \end{pmatrix}, \quad \mathbf{C}_n = \begin{pmatrix} \frac{2n-1}{n+1} & -\frac{n-2}{n+1} \\ 1 & 0 \end{pmatrix}, \quad \mathbf{B}_n = \begin{pmatrix} -h^2 b_n^* \\ 0 \end{pmatrix},$$

where

$$b_n^* = -\frac{e_{n+2} - \frac{2n-1}{n+1}e_{n+1} + \frac{n-2}{n+1}e_n}{h^2} = b_n - \frac{L[x(t_{n+1}); h]}{h^2}.$$

Then (C.1) can be written as

$$\mathbf{E}_{n+1} = \mathbf{C}_n \mathbf{E}_n + \mathbf{B}_n.$$

By recursive method, we have

$$\mathbf{E}_n = \mathbf{C}_{n-1} \cdots \mathbf{C}_0 \mathbf{E}_0 + \sum_{l=1}^n \mathbf{C}_{n-1} \cdots \mathbf{C}_{n-l+1} \mathbf{B}_{n-l}.$$

With the notations introduced in Lemma 2, this equality can be written as

$$\mathbf{E}_n = \mathbf{D}_{n-1,n} \mathbf{E}_0 + \sum_{l=1}^n \mathbf{D}_{n-1,l-1} \mathbf{B}_{n-l}. \quad (\text{C.3})$$

Now we need to estimate $\|\mathbf{B}_n\|$. From (C.2) and the L -Lipschitz property of ∇F , we have

$$|b_n| \leq L \left(\frac{2n-1}{n+1} |e_{n+1}| + \frac{n-2}{n+1} |e_n| \right) \leq L(2|e_{n+1}| + |e_n|) \leq 3L \|\mathbf{E}_n\|$$

and

$$\|\mathbf{B}_n\| \leq 3h^2 L \|\mathbf{E}_n\| + L[x(t_{n+1}); h]. \quad (\text{C.4})$$

Taking norm on both sides of (C.3) and substituting (C.4) and conclusion of Lemma 2 yields

$$\begin{aligned} \|\mathbf{E}_n\| &\leq M_3 \|\mathbf{E}_0\| + M(n-1) \sum_{l=0}^{n-1} (3h^2 L \|\mathbf{E}_l\| + L[x(t_{l+1}); h]) \\ &\leq M_3 \|\mathbf{E}_0\| + 3Mnh^2 L \sum_{l=0}^{n-1} \|\mathbf{E}_l\| + Mn \sum_{l=0}^{n-1} L[x(t_{l+1}); h]. \end{aligned} \quad (\text{C.5})$$

Now we deal with truncation errors. Recall (A.3) in Remark 3 of Theorem 1

$$|L[x(t_l); h]| \leq M_1 h^3 + M_2 \frac{h^2}{l}.$$

Take sum to obtain

$$\sum_{l=0}^{n-1} |L[x(t_{l+1}); h]| \leq nM_1 h^3 + M_2 h^2 \sum_{l=0}^{n-1} \frac{1}{l+1}. \quad (\text{C.6})$$

In addition, we have the classic inequality

$$\sum_{i=1}^n \frac{1}{i} \leq \ln n + M_e,$$

where M_e refers to a positive constant. We substitute it to (C.6) to get

$$\sum_{l=0}^{n-1} |L[x(t_{l+1}); h]| \leq nM_1h^3 + M_2h^2(\ln n + M_e).$$

Then we substitute this inequality to (C.5) to get a control of $\|\mathbf{E}_n\|$

$$\|\mathbf{E}_n\| \leq M_3\|\mathbf{E}_0\| + 3Mnh^2L \sum_{l=0}^{n-1} \|\mathbf{E}_l\| + MM_1n^2h^3 + MM_2M_e nh^2 + MM_2nh^2 \ln n.$$

Using discrete Gronwall inequality, we have

$$\|\mathbf{E}_n\| \leq e^{3Mn^2h^2L} (M_3\|\mathbf{E}_0\| + MM_1n^2h^3 + MM_2M_e nh^2 + MM_2nh^2 \ln n + 3Mnh^2L\|\mathbf{E}_0\|).$$

Then for fixed t , from the relation $n = \frac{t}{h}$ we get

$$\|\mathbf{E}_{t/h}\| \leq e^{3Mt^2L} \left((M_3 + 3MthL)\|\mathbf{E}_0\| + (MM_1t^2 + MM_2M_e t)h + MM_2th \ln \frac{t}{h} \right).$$

Notice that

$$\lim_{h \rightarrow 0} h \ln \frac{t}{h} = 0.$$

So if $\mathbf{E}_0 = \mathbf{0}$, then the vector form of overall error $\mathbf{E}_{t/h}$ satisfies

$$\lim_{h \rightarrow 0} \|\mathbf{E}_{t/h}\| = 0.$$

More precisely, we have

$$\|\mathbf{E}_{t/h}\| = \mathcal{O}\left(h \ln \frac{1}{h}\right),$$

for $h \rightarrow 0$. □

D Proof of Theorem 3

Theorem 3. If ∇F has continuous second order derivative, the first and second derivative are bounded, and $x(t)$ has continuous fourth derivative, then for fixed t , truncation error of SAG (3.1) satisfies

$$L[x(t); h] = \mathcal{O}(h^4).$$

Proof. Recall the proof of Theorem 1. Now we expand $x(t-h)$ to first order

$$x(t-h) = x(t) + hx^{(1)}(t) + \mathcal{O}(h^2).$$

Then we have

$$\begin{aligned}
& \nabla F \left(x(t) + \frac{t-3h}{t}(x(t) - x(t-h)) \right) \\
&= \nabla F \left(x(t) + \left(1 - \frac{3h}{t}\right)(hx^{(1)}(t) + \mathcal{O}(h^2)) \right) \\
&= \nabla F \left(x(t) + hx^{(1)}(t) + \mathcal{O}(h^2) \right) \\
&\stackrel{(1)}{=} \nabla F \left(x(t) + hx^{(1)}(t) \right) + \mathcal{O}(h^2) \\
&\stackrel{(2)}{=} \nabla F(x(t)) + \nabla^2 F(x(t)) \left(hx^{(1)}(t) \right) + \mathcal{O}(h^2) \\
&= \nabla F(x(t)) + h \cdot \nabla^2 F(x(t)) \cdot x^{(1)}(t) + \mathcal{O}(h^2).
\end{aligned} \tag{D.1}$$

In the (1) equality, we use the L -Lipschitz property of ∇F . In the (2) equality, we expand ∇F to second order. To do this, we need ∇F has continuous second derivative and the second derivative is bounded.

Then we take derivative on both sides of differential equation

$$x^{(2)}(t) + \frac{3}{t}x^{(1)}(t) + \nabla F(x(t)) = 0$$

to get

$$\nabla^2 F(x(t)) \cdot x^{(1)}(t) = \frac{d}{dt}(\nabla F(x(t))) = -x^{(3)}(t) - \frac{3}{t}x^{(2)}(t) + \frac{3}{t^2}x^{(1)}(t). \tag{D.2}$$

The differential equation can also be written as

$$\nabla F(x(t)) = -x^{(2)}(t) - \frac{3}{t}x^{(1)}(t). \tag{D.3}$$

We substitute (D.2) and (D.3) to (D.1) to get

$$\begin{aligned}
\nabla F \left(x(t) + \frac{t-3h}{t}(x(t) - x(t-h)) \right) &= -hx^{(3)}(t) - \left(\frac{3h}{t} + 1 \right) x^{(2)}(t) \\
&\quad + \left(\frac{3h}{t^2} - \frac{3}{t} \right) x^{(1)}(t) + \mathcal{O}(h^2).
\end{aligned} \tag{D.4}$$

We expand $x(t+h)$, $x(t-h)$, $x(t-2h)$ to the third order

$$\begin{aligned}
\left(\alpha_1 + \frac{\beta_1 h}{t} + \frac{\gamma_1 h^2}{t^2}\right) x(t+h) &= \left(\alpha_1 + \frac{\beta_1 h}{t} + \frac{\gamma_1 h^2}{t^2}\right) \\
&\quad \left[x(t) + hx^{(1)}(t) + \frac{h^2}{2}x^{(2)}(t) + \frac{h^3}{6}x^{(3)}(t) + O(h^4) \right], \\
\left(\alpha_3 + \frac{\beta_3 h}{t} + \frac{\gamma_3 h^2}{t^2}\right) x(t-h) &= \left(\alpha_3 + \frac{\beta_3 h}{t} + \frac{\gamma_3 h^2}{t^2}\right) \\
&\quad \left[x(t) - hx^{(1)}(t) + \frac{h^2}{2}x^{(2)}(t) - \frac{h^3}{6}x^{(3)}(t) + O(h^4) \right], \\
\left(\alpha_4 + \frac{\beta_4 h}{t} + \frac{\gamma_4 h^2}{t^2}\right) x(t-2h) &= \left(\alpha_4 + \frac{\beta_4 h}{t} + \frac{\gamma_4 h^2}{t^2}\right) \\
&\quad \left[x(t) - 2hx^{(1)}(t) + 2h^2x^{(2)}(t) - \frac{4h^3}{3}x^{(3)}(t) + O(h^4) \right].
\end{aligned}$$

Now we substitute these three equations and (D.4) to truncation error of recurrence relation (3.1)

$$\begin{aligned}
L[x(t); h] &= \sum_{i=1}^4 \left(\alpha_i + \frac{\beta_i h}{t} + \frac{\gamma_i h^2}{t^2} \right) x(t + (2-i)h) \\
&\quad + h^2 \nabla F \left(x(t) + \frac{t-3h}{t} (x(t) - x(t-h)) \right).
\end{aligned}$$

Simple calculation shows that terms with order less than four will be eliminated if and only if the following equations are satisfied,

$$\begin{cases} \alpha_1 = 2 \\ \alpha_2 = -5 \\ \alpha_3 = 4 \\ \alpha_4 = -1 \end{cases}, \quad \begin{cases} \beta_1 = \frac{9}{2} - k \\ \beta_2 = -6 + 3k \\ \beta_3 = \frac{3}{2} - 3k \\ \beta_4 = k \end{cases}, \quad \begin{cases} \gamma_1 = m_1 \\ \gamma_2 = -\frac{3m_1 + m_2 + 3}{2} \\ \gamma_3 = m_2 \\ \gamma_4 = \frac{m_1 - m_2 + 3}{2} \end{cases},$$

where k , m_1 , m_2 can be chosen randomly. Then we set $k = \frac{1}{2}$, $m_1 = 0$ and $m_2 = 3$ to get our SAG (3.1). \square

E Algorithms for matrix completion experiment

In this section we present FISTA (Algorithm 4), APG (Algorithm 5), FISTA with backtracking (Algorithm 6) and APG with backtracking (Algorithm 7).

F Detailed experiment results

We use cross-entropy loss to train the network for handwriting digit recognition task. In every iteration of the two methods, we calculate the gradient using all the 20000 training images, so it

Algorithm 4 FISTA

Input: step size s .

Initial value: $\mathbf{Y}_1 = \mathbf{X}_0 = \mathbf{M}_{obs}$, $t_1 = 1$.

k th iteration ($k \geq 1$). Compute

$$\begin{aligned}\mathbf{X}_k &= \arg \min_{\mathbf{X}} \left\{ \frac{1}{2s} \|\mathbf{X} - (\mathbf{Y}_k - sg(\mathbf{Y}_k))\|^2 + \lambda \|\mathbf{X}\|_* \right\}, \\ t_{k+1} &= \frac{1 + \sqrt{1 + 4t_k^2}}{2}, \\ \mathbf{Y}_{k+1} &= \mathbf{X}_k + \frac{t_k - 1}{t_{k+1}} (\mathbf{X}_k - \mathbf{X}_{k-1}).\end{aligned}$$

Algorithm 5 Accelerated proximal gradient method (APG)

Input: step size s .

Initial value: $\mathbf{X}_1 = \mathbf{X}_0 = \mathbf{M}_{obs}$.

k th iteration ($k \geq 1$). Compute

$$\begin{aligned}\mathbf{Y}_k &= \mathbf{X}_k + \frac{k-3}{k} (\mathbf{X}_k - \mathbf{X}_{k-1}), \\ \mathbf{X}_{k+1} &= \arg \min_{\mathbf{X}} \left\{ \frac{1}{2s} \|\mathbf{X} - (\mathbf{Y}_k - sg(\mathbf{Y}_k))\|^2 + \lambda \|\mathbf{X}\|_* \right\}.\end{aligned}$$

Algorithm 6 FISTA with backtracking

Input: some $\beta < 1$.

Initial value: $\mathbf{Y}_1 = \mathbf{X}_0 = \mathbf{M}_{obs}$, $t_1 = 1$, step size s_0 .

k th iteration ($k \geq 1$).

Find the smallest nonnegative integer i_k such that with $s = \beta^{i_k} s_{k-1}$

$$F(\widetilde{\mathbf{X}}) < F(\mathbf{Y}_k) + \left\langle \widetilde{\mathbf{X}} - \mathbf{Y}_k, g(\mathbf{Y}_k) \right\rangle + \frac{1}{2s} \|\widetilde{\mathbf{X}} - \mathbf{Y}_k\|^2,$$

where

$$\widetilde{\mathbf{X}} = \arg \min_{\mathbf{X}} \left\{ \frac{1}{2s} \|\mathbf{X} - (\mathbf{Y}_k - sg(\mathbf{Y}_k))\|^2 + \lambda \|\mathbf{X}\|_* \right\}.$$

Set $s_k = \beta^{i_k} s_{k-1}$ and compute

$$\begin{aligned}\mathbf{X}_k &= \widetilde{\mathbf{X}}, \\ t_{k+1} &= \frac{1 + \sqrt{1 + 4t_k^2}}{2}, \\ \mathbf{Y}_{k+1} &= \mathbf{X}_k + \frac{t_k - 1}{t_{k+1}} (\mathbf{X}_k - \mathbf{X}_{k-1}).\end{aligned}$$

Algorithm 7 APG with backtracking

Input: some $\beta < 1$.

Initial value: $\mathbf{X}_1 = \mathbf{X}_0 = \mathbf{M}_{obs}$, step size s_1 .

k th iteration ($k \geq 1$). Compute

$$\mathbf{Y}_k = \mathbf{X}_k + \frac{k-3}{k}(\mathbf{X}_k - \mathbf{X}_{k-1}).$$

Find the smallest nonnegative integer i_{k+1} such that with $s = \beta^{i_{k+1}} s_k$

$$F(\tilde{\mathbf{X}}) < F(\mathbf{Y}_k) + \langle \tilde{\mathbf{X}} - \mathbf{Y}_k, g(\mathbf{Y}_k) \rangle + \frac{1}{2s} \|\tilde{\mathbf{X}} - \mathbf{Y}_k\|^2,$$

where

$$\tilde{\mathbf{X}} = \arg \min_{\mathbf{X}} \left\{ \frac{1}{2s} \|\mathbf{X} - (\mathbf{Y}_k - sg(\mathbf{Y}_k))\|^2 + \lambda \|\mathbf{X}\|_* \right\}.$$

Set $s_{k+1} = \beta^{i_{k+1}} s_k$ and compute

$$\mathbf{X}_{k+1} = \tilde{\mathbf{X}}.$$

is meaningful to study the change of the training loss during iteration. In Figure 3 we plot the training loss against the number of iterations for SAG and NAG. This figure also shows that SAG is more stable than NAG when step size is large.

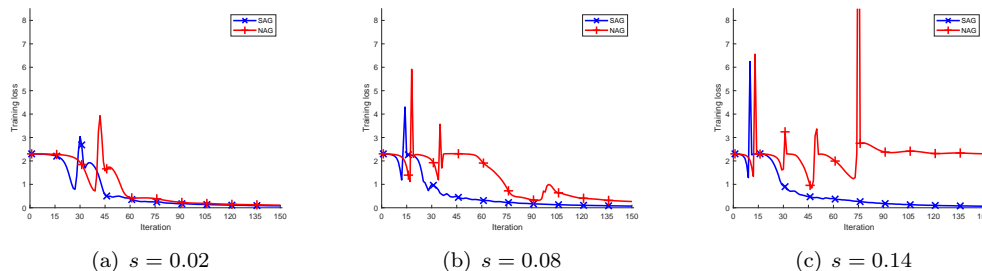


Figure 3: Iterations of SAG and NAG for training loss. Y-axis represents the training loss for both methods. Step sizes for the three subgraphs are 0.02, 0.08 and 0.14, coinciding with Figure 2.